QUANSE 2002
International Congress on
Quality Assessment of Numerical Simulations in Engineering
April 9-12-2002
University of Concepción - Chile

QUANSE 2002 – Finite Element Model Updating of Plate-like Structures Using Modal Holographic Measurement Field

D. Simon*, J-C. Golinval

ASMA - Vibrations et Identification des Structures
University of Liège, Liège, Belgique
e-mail: d.simon@ulg.ac.be

Key words: blades, field measurement techniques, updating.

Abstract

Optical measurement techniques are very promising for finite element (F.E.) model updating or error localisation of plate-like structures in the field of structural dynamics. The purpose of this work is to investigate a way to better exploit the high spatial resolution inherent to these techniques in order to correct FE mesh discretisation errors and/or model parameter errors. An important assumption in F.E. model error detection is first to consider the initial mesh as sufficiently fine to well represent the measured (displacement or stress) field. In the case of model updating, the adjustment of the model is performed by minimising the difference between the outputs of the model and the exact solution with respect to design parameters. In the case of FE mesh adaptation, the exact solution has to be estimated whereas in the case of model parameter errors, the reference solution is assumed to be the measured one. The idea developed in this paper is to take advantage of the high spatial resolution offered by optical techniques to calculate successively two error estimators using only measurements. The experimental field is first used for the detection of singular regions corresponding to high gradients. This estimator indicates the regions where a mesh refinement is required. Thus a second estimator is calculated and used for parameter error detection.

1 Introduction

The study of jet engine turbine's blades constitutes a very interesting field of investigation for researchers working in structural dynamics.
Industrials are looking for more accurate dynamical behaviour predictions. But blades have been studied for years and industry is confronted with current experimental and analytical techniques approaching the end of their development. On the other side, the development cost and the importance (as much strategic as technical) of turbine blades justify the development of new technologies and heavy studies. Of course, cost and lead-time are of major importance. It seems that innovations in the study of blade dynamical behaviour must go through a better exploitation of experimental results and the implementation of new testing processes.

1.1 Specific dynamics problems of turbine blades

In a jet engine, rotating components (i.e. rotor blades) passing in front of fixed components (i.e. stator blades) are excited by important pressure fluctuations. The number of blades on a stage and the combinations between stages generate excitations acting on a wide frequency band (up to 20 kHz) during engine's normal operating rotation speeds. Up to twenty vibrating modes may be excited on a blade and they become a potential cause of failure during operation.

Blades have been modelled using the Finite Element Method (F.E.M.) since the beginning of commercial software. This process has been well dominated for years. The main problem is not coming from the reliability of the F.E. used for the – virtual – modelling, but from the physical behaviour of a blade. This one has been manufactured with tolerances, with local heating, stresses or it has perhaps been used, tested or damaged. This reality is included in the model via safety coefficients. The use of lighter, higher performance blades with less conservative margins of safety requires a better model of the real blade, not the virtual one. This can be achieved with dynamic testing, fault detection and model updating. In this paper, we will focus on the dynamic testing and F.E. model improvement process of compressor blades.

1.2 Dynamic testing objectives

When dealing with jet engine blades, which are excited at high-frequencies, dynamic testing programs are very difficult to achieve.
The first objective is the detection of very small size structural faults for the updating at the modelling level. The second goal is to determine optimum sensor placement for the monitoring of all critical vibratory responses within the wide engine excitation range, to avoid unexpected resonances encountered during initial and costly engine running. Due to the number of locations necessary and the engine instrumentation limitations, it is not possible to measure maximum stress for all responses. In order to monitor dynamics stress or displacement for all critical vibratory response modes, the sensors location have to be optimally selected to measure a significant percentage of the maximum stress of all modes of interest. During dynamic testing, ratio have to be established between maximum stress or displacement locations and optimum nominal engine sensors locations. For structural health monitoring or for quality control the objective is to detect out of tolerance parameters or minor damages before they can combine and propagate to cause failure of the blade.
Of course, accessibility to the blade is required for a short time and non destructive techniques have to be used.

1.3 Particularities of blades dynamic testing

To achieve those objectives, complex high frequency modes have to be analysed because they are more sensitive to damage than simpler lower frequency modes. This leads to high spatial resolution measurement techniques.
Problems arise due to technical limitations, especially for light weight structures measurements. The use of distributed sensors (e.g. accelerometers) in dynamic structural testing is a widespread measurement technique. However, it usually leads to a very poor spatial resolution. The large number of measurement points which is needed would require too many sensors to be placed on the structure under test. This not only gives practical problems, but also technical ones such as mass loading effects. Moreover, in the medium to high frequency range the wavelength of the structural motion is in the range of the distance between two neighbouring sensors or even of their diameter.
In conclusion, the experimental techniques used for dynamic testing have to be able to measure a full field of deformations of the vibrating structure in a non-contact and punctual way on a very wide frequency band with a high sensitivity.

2 The errors in a F.E. models

Considering that capabilities of numerical structural modelling are increasing, the analyst do not readily admit that the models may contain inaccuracies, while the reality is that these models are approximations of what he believes the system to be. Models need to be adjusted, refined and broadened to provide a better representation of the real system. Different types of errors may arise in F.E. models:
Errors associated with discretisation in model generation. They are related to the number of elements, to their type and their spatial distribution.
Idealisation errors in the model assumptions. They are associated to uncertainty on the boundary conditions and inaccuracy in the idealisation of the model parameters.
Errors associated to model updating. They are related to the critical steps -expansion, parameters selection – of the process. The selection of the elements and their characteristics, which are allowed to change, and the range of variation are of major importance. If the wrong parameters are selected for updating then an incorrect description of the updated model may result. The analyst understanding of the model and selection of parameters are heavily dependent on the location and type of detected discrepancies. However, the quality of the error localisation strongly depends on the expansion reliability, which is itself related to the number of well identified experimental modes. In fact the main drawback of mode-shape vector expansion techniques is that mathematical errors due to the expansion process are spread all over the structure. They are added to measurement errors and noise. A large number of measured co-ordinates helps to enhance the expansion quality and thus the model error localisation results.
Errors inherent to numerical operations.

3 Appropriate experimental techniques

Particularities of turbine blade dynamic testing – full field, non-contact, punctual deformation measurement – require new experimental techniques. These can be divided in two categories; those measuring a strain field –thermographic and/or thermoelastic strain measurement – and those, very sensitive, measuring a displacement field by use of a laser illumination (Holographic Interferometry and Electronic Speckle Pattern Interferometry (ESPI)) – Scanning Laser Doppler Vibrometry (SLDV).

Field measurement techniques offers many opportunities to increase the investigation capabilities of experimental vibration testing. Nevertheless, their use introduces new problems with respect to traditional measurement techniques. Despite great technical advances, their use in the field of modal analysis is still quite limited. In fact, some technical problems are not yet completely solved.

3.1 SLDV

The Laser Doppler Velocymetry (LDV) is a non-contact velocity transducer based on the analysis of Doppler effect on a laser beam emerging from a moving surface. It offers the possibility of performing quick and flexible non-intrusive vibration measurements.

LDV's major advantage compared with other optical techniques is its ability to measure not only harmonic but also random vibrations. This allows a quick measure on a wide frequency band of response functions and the use of classical identification programs. The very large range of vibration amplitude can also be an advantage. By means of a scanning system (composed of two mirrors with orthogonal rotation axes which deflect the focused laser beam in the desired location), the measurement beam can rapidly, precisely and automatically be positioned from point to point. This is different of the other techniques mentioned above which provide a simultaneous measure of the points on the surface and display a digital picture.
Recent commercial systems are already able to pilot the measurement point on a geometrical 3-D grid with a high spatial resolution [15]. In-plane and out-of-plane velocity components at a point are determined. The knowledge of a hihgh3-D spatial density field can be used to determine many dynamic properties such as rotations, strains, stress and acoustic emissions. [13] used changes in curvatures of the Operational Deflection Shapes (ODS) of a blade to locate the damage. A SLDV measures the vibration while piezoceramic patches provide the excitation.
Therefore, and this is true for all optical measurement techniques, LDV is sensitive to many interfering inputs : optical properties and roughness of the measured specimen, density of the medium where the optical beam propagates. Problems may arise from the control and use of automatic scanning [14].

3.2 Thermography – thermoelacticity

The thermoelastic effect is the adiabatic temperature change due to material dilatation. This small and local temperature variations are measured with an infrared camera. [11] used experimental thermoelastic analysis on high frequency modes of vibration of a complex turbine impeller and outlined problems with vibrating modes resulting in high multi-axial stress distribution. The system displays stress magnitude based on the sum of its principal stress values, which could be significantly higher than either of the individual principal stresses. Since strain gage output indicates stress only in the direction of strain orientation, this discrepancy with thermoelastic results is a problem for optimum strain gage locations. Moreover, the possible incompatibility between strain gage size the spatial resolution has to be considered.
The main limitation in this technique for vibration response measurement is the stress level required especially for high frequencies.
The thermoelastic stress measurement is not strictly speaking a non-contact technique when a thick coating has to be applied on the measured surface. This can influence high frequencies of light structure vibration response.

3.3 Interferometry

Together with LSDV, interferometry techniques, such as Electronic (or Digital) Speckle Pattern Interferometry (ESPI or DSPI) or holographic interferometry, look the most promising.

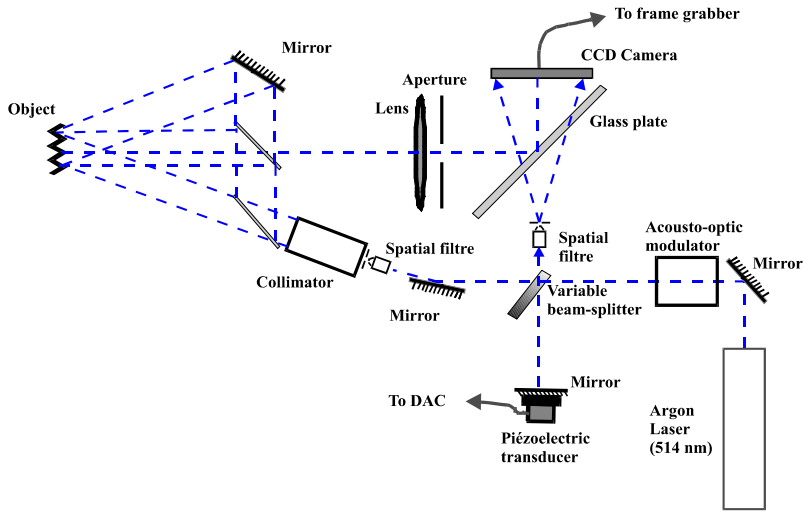

Figure 1 : *DSPI set-up*

Speckle is the grainy aspect of the image produced by coherent light illuminating an optically rough surface. The speckle is moving with the illuminated surface. The recording of the interference between the speckle pattern and a reference beam (called "specklegram") enables to measure the displacement of the surface. When the surface gets out of shape, an optical path difference (OPD) occurs in the interferometer (***fig . 1***). The OPD is recorded by a CCD camera as a variation of the speckle intensity. The subtraction of the phase associated at each object point before and after object displacement yields a fringe pattern. When interferences between two exposures of a moving surface taken at different moments in time are generated, the fringes (alternation of dark and bright areas) represent contour lines of displacement which occurred between the two exposures.

The recording of three OPDs along three sensitivity directions enables to extract the 3-D displacement at each point of the surface. The three sensitivity directions are the bisecting lines of the angles formed with optical axis of the visualization system and the three object beams that illuminate the object under investigation. During the acquisition process, the object is illuminated with each object beam alone so that three measurements are necessary to determine the 3-D displacements [9].

DSPI used a CCD camera to produce and analyse the fringe map. In holographic interferomerty, it is neccessary to record again the holographic interferograms witk the CCD camera. The DSPI system is less sensitive to perturbations because of its lower resolution.

A very common technique to measure harmonic vibration with interferometry is the time-averaging technique instead: of measuring the interference between two moments in time, interference between a rest state and a recording of several periods are gathered and averaged. This technique is used very often as a quick but rough modal analysis method where a sine wave generator is controlled and swept in frequency. As the camera gives the fringe pattern in real time, it is very easy to find the resonance frequencies and to get an idea of the deformation shape. But only the amplitude of the sinusoidal vibration at each point can be measured. Any phase information is lost. By using phase shifting technique, and stroboscopic laser illumination at the vibration frequency, it is possible to extract amplitude and phase information for every point (pixel) of the fringe pattern at a single frequency. The strobing pulse is synchronised with the excitation signal ensuring that maxima or minima of the surface motion are observed. An interferogram between the image of the structure without excitation and an image of the vibrating structure is recorded. This process obviously assumes a response field with all displacements perfectly in phase.

3.4 Differentiating close modes

Waiting for the use of time pulsed laser, holographic measurement techniques are only able to deal with an harmonic vibration at a constant frequency. The complete set of complex FRF's necessary for modal parameters identification is not available.
[12] have rebuilt FRF using as many hologram recordings as spectral lines in the target frequency band. When all FRFs are measured and calculated, standard modal parameters identification methods can be used. But this process is very heavy and, due to the high number of available response points, the modal parameter estimation methods might be optimised which leads to spatial domain techniques.
So, the state of the art in holographic vibration measurement for experimental modal analysis implicates the following major assumption : the structure vibrates in a mode where only one mode shape is present. This is even extended to the constraint that this single mode is excited with only one harmonic excitation signal at resonance frequency. This is equivalent to assume that a response deformation shape due to a single harmonic excitation at resonance frequency is equal to a mode shape.

$$\boldsymbol{z}_{(k)} = \boldsymbol{x}_{(k)} + \sum_{\substack{s=1 \\ s \neq k}}^{n} i \;\; \omega_{0k} \frac{\beta_{ks}}{\mu_s \;\; (\;\; \omega_{0k}^2 \;\; - \;\; \omega_{0k}^2 \;\;)} \boldsymbol{x}_{(s)} \qquad (1.)$$

$$a_{kl}(i\omega) = \sum_{s=1}^{n} \frac{1}{(\;\; \omega_{0s}^2 - \omega^2 + 2 \;\; i \;\; \varepsilon_s \;\; \omega \;\; \omega_{0s} \;\;)} \frac{x_{k(s)} \;\; x_{l(s)}}{\mu_s} \qquad (2.)$$

Equations for the harmonic response vector $z_{(k)}$ and dynamic influence coefficients a_{kl} show that the above statement is true if :
- The natural frequencies of the modes are far from each others. Then, the modal response to all modes is low compared to the modal response of the target mode k.
- The damping is low.
- The forcing vector is such as it amplifies the mode *k* and attenuates all other ones.

Otherwise, the response displacement at a natural frequency will be contaminated by other mode shapes. The combination of mode shapes will also result in a response displacement where all points do not move in phase. This phase difference can not be detected by time-averaged method.
For larger blades, a multi-exciter sinusoidal excitation where the forces are tuned to force a pure normal mode behaviour could be a solution. Piezoceramic patches could provide the excitation. But simple recommendations can also improve efficiency of holographic measurements for experimental modal analysis :
- Use of a force control to guarantee a constant response displacement.
- Introduction of a load cell to measure input force and some reference responses. One accelerometer for the driving point and a LDV for resonance frequencies detection and, if necessary, for a very rough identification of damping ratio.

[14] develops techniques to solve other technical points to be considered before using the optical data in a F.E.M. updating process.

4 Exploiting experimental data

Since the interferometry based measurement techniques output displays a coarse 2D grid of points (up to 512 x 512) compared with the 3-D finite element analysis results, the major difficulty is no more the lack of experimental information but the way to manage the measurement field to their best.
The challenge is the transformation of measurements of a physical phenomenon into values compatible with theoretical hypotheses associated to F.E. modelling - for example discontinuity of the

stress field, degree of the displacement field – and defined on a mesh to give them a meaning in the F.E. technique point of view. Experimental stress values are seldom used for finite element model improvement, because of the difficulty to introduce stress data in standard updating schemes.[4] chose a mixed finite element approach, based on simultaneous approximation of displacement and stress field to overcome that problem.
When the measured and calculated values are of same nature and associated to the same topology, the analytical vs. experimental discrepancy is easy to determine. At this point, one would like to be able to compare the measured value at each pixel with the corresponding value of the discretised solution. However, the transformation of the experimental data (defined in the absolute reference frame) into the intrinsic coordinates system of a single finite element is a difficult inverse problem. Moreover, the stress field is not continuous in the kinematically acceptable models. For these reasons, it is preferable to fit the experimental field using the same polynomial expressions as the ones used in the finite element formulation. [4] has chosen to transform experimental value into a modal vector for each element. To associate experimental measurement points coordinates with values in the intrinsic co-ordinate system, each element has to be divided in small areas where the experimental value is assumed to be constant. Nodal values are computed through interpolation functions of the same degree as the finite element modelling. This attractive technique implicitly supposes that, on each element, the experimental field can be expressed by a polynomial expression of the same degree as the F.E. representation. In other words, it supposes that the discretisation is sufficiently fine to precisely represent the experimental field.
But if mesh refinement techniques are very efficient to build models which represent well what the modelled structure is expected to be, they are not able to take into account what measurements reveal it is in reality.

5 Original solution

The idea is to start by comparing the experimental field with the F.E. one. The experimental field is introduced in a mesh discretisation error calculation process. This permits the detection of singular regions corresponding to high gradients. When the mesh is refined to be able to represent the experimental field with a given precision, the latter is transformed into modal vectors can be used in the updating process.
The similitudes between the indicators used in discretisation error detection and in the updating processes make this approach much more easier. Indeed, common error localisation common methods [Ph Colignon] used for updating and failure detection use a residual energy indicator. It consists in evaluating the residual energy at a local level (element-by-element or substructure-by substructure). The error estimate for element *e* corresponding to mode *k* is given by :

$$e^{e}_{(k)} = \left(\{V^e\}_{(k)} - \{U^e\}_{(k)} \right)^T [K^e] \left(\{V^e\}_{(k)} - \{U^e\}_{(k)} \right) \qquad (3.)$$

where $\{V\}$ represents the experimental eigen mode, $\{U\}$ the analytic one and $[K]$ the stiffness matrix.

The global error estimate for element *e* is obtained from : $E^e = \sum_{k=1}^{m} e^{e}_{(k)}$ *(4.)*

where *m* is the total number of measured modes.

Equation *(3.)* is in fact equation: $\int_{V_e} \| [D][\nabla]\{u\} - [D][\nabla]\{v\} \| \, dV_e$ *(5.)*

where the metric *[D]* $^{-1}$, Euclidian norm and the dicretised expression of the displacement field *(6.)* have been used.

$$\{ u(x,y,z) \} = \sum_{i=1}^{n} N_i^e \begin{Bmatrix} u_i \\ v_i \\ w_i \end{Bmatrix} = N^e \{U^e\} \qquad (6.)$$

where ∇ is the spatial differentiation operator and *D* the elasticity matrix. *N* is the shape function and U^e the vector for generalised coordinates resulting from the finite element discretisation of the structure.
This is equivalent to evaluate the distance between two stress fields :

$$\int_{V_e} \| \{\sigma\} - \{\lambda\} \| \, dV^e \qquad (7.)$$

where σ is the experimental or reference field associated with the corresponding mode shape vector *u* and λ is the analytical stress field associated to *v*
This expression used here for the localisation of discrepancies between analytical and experimental results is also the basis of some mesh refinement methods in static linear analysis. Actually, it is well known that the use of a kinematically admissible FE model leads to residual errors in the equilibrium equation and to stress discontinuities along the interfaces between the elements. Mesh refinement methods [1,3] look to transform these errors into an indicator of discretisation errors. The error estimation methods based on the discontinuity of the finite element's solution stress field, consists in building a new field with better continuity properties from this solution. This improved field replace directly the experimental field in equation *(7.)*.
The elements' new size are determined on the basis of the global error, of the local errors provided from the estimator and of a convergence ratio of the solution in the elements. Then a new mesh can be generated.

5.1 Analogy with mesh discretization errors detection

Our fault detection methodology is established by analogy with mesh refinement techniques studied by Dufeu-Beckers [3].
The method used to lead to the field λ consists in building a field with a degree at least one time greater than the finite element analysis one. This field may be expressed at an element level following:

$$\tilde{\varphi} = \sum_{i=1}^{n} N_i \, \tilde{s}_i \qquad (8.)$$

where *n* is the number of measurement points included on the element skin, N_i is a polynomial function with the same degree as the field and $\tilde{s}_i$ the experimental values. To ensure that the field is continuous, $\tilde{\varphi}$ will take the form of a polynomial function defined on an area Ω_r of the measured domain.

5.2 Representation of the field

Whether speaking about the displacement or the stress field, the notation φ_r will be used to represent the recovered field. Each component of this field is represented by the polynomial function:

$$\tilde{\varphi} = P_n(\chi)a \qquad (9.)$$

with

$$P_n(\chi)a = \sum_{i=1}^{T_n} \left(x^j\ y^k\ z^l\right)_i\ a_i \qquad j+k+l \le n \qquad (10.)$$

where the number of terms is equal to : $T_n = \dfrac{(n+1)(n+2)(n+3)}{6}$

This approach is compatible with all the new field measurement techniques introduced above because φ can be a stress, strain or displacement field.

5.3 Definition of the patch area

The patches are the areas drawn by the projection on the measurement grid of several finite elements and in general, they overlap partly. These areas must be chosen to have enough data to allow the interpolation of the field. The fields φ_r will be built on those areas. Usually, the patch area associated to a node j is made up of the set of elements that are connected to this node. But a patch can be associated to an element. This method is known as the “patch recovery” method

$$\Omega_{rj} = \bigcup_{i=1}^{m_j} \Omega_i \qquad (11.)$$

where Ω_i represents the element i and m_j the number of elements connected to the node j.

The nodes taken into account to build the patches are only those defining an element face which contain measured points. Here a patch is a 3-D surface and not a volume.

5.4 Normalisation of the coordinates

It is shown in [7] that the results of the recovery of a field represented by a bilinear polynomial depend on the co-ordinate system of the area, on its position, on its size and its orientation. In order to obtain the most general possible procedure, it is necessary to have a recovery method that is independent of the system of axes chosen to evaluate the polynomial coefficients. It has been shown in reference [3] that it is advisable to use a complete polynomial and a normalised system of coordinates. The normalisation used in one axis is defined in the space *[-1,1]* by:

$$\chi_n = -1 + 2\frac{\chi - \chi_{\min}}{\chi_{\max} - \chi_{\min}}$$ where χ represents the co-ordinates.

This normalisation guarantees the definition of an area which touches all the lines defining the limits of the normalised space [3] and which is weakly dependent on a particular direction.

5.5 Construction of the field φ_r

The unknown parameters *a* in equation *(9.)* are obtained by minimisation of the difference between the experimental results and the smoothed values at the points of measurement in the "patch". This results in minimising the function :

$$\omega(x_i, y_i, z_i)\left(\varphi_r(x_i, y_i, z_i) - \varphi_{EXP}(x_i, y_i, z_i)\right) \qquad (12.)$$

$$\omega(x_i, y_i, z_i)\left(P_n(x_i, y_i, z_i)\, a - \varphi_{EXP}(x_i, y_i, z_i)\right) \qquad (13.)$$

or

$$R_i(a) = 0 \qquad (14.)$$

where $\omega(x_i, y_i, z_i)$ is a weighting function that can be used to balance the influence of the points (x_i, y_i, z_i) according to their distance to the central node which defines the geometrical area. The problem defined by equation *(14.)* is in general over-determined and its solution can be estimated using a least square method. For this purpose, let us consider the following function :

$$F_i(a) = \sum_{i=1}^{m_i} \left(R_i(x_i, y_i, z_i)\right)^T \left(R_i(x_i, y_i, z_i)\right) \qquad (15.)$$

where (x_i, y_i, z_i) are the coordinates of the selected group of points; $m_i = \sum_e k_e$ is the total number of these points (k_e = the number of points in an element of the area).

The minimisation procedure $\frac{\partial F(a)}{\partial a} = 0$ leads to the system of equations [Dufeu] :

$$\sum_{i=1}^{m_i} \omega^2(x_i, y_i, z_i)\, P_n^T(x_i, y_i, z_i)\, P_n(x_i, y_i, z_i)\, a = \sum_{i=1}^{m_i} \omega^2(x_i, y_i, z_i)\, P_n^T(x_i, y_i, z_i)\, \varphi_{EXP}(x_i, y_i, z_i) \qquad (16.)$$

which can be put in the matrix form:

$$\{a\} = [A]^{-1}\{b\} \qquad (17.)$$

Note that the number of equations to be solved for each component in each area is low. This makes the method less expensive than a method that would use a global projection. It should be noted that this construction process leads to a smoothed experimental field. It will be explained later that this can be an advantage. However, the difference between this improved field and the experimental one can be quantified at a previous stage when the FE mesh quality is checked. If the FE model discretisation of the structure is well adapted, the difference between the two fields is weak.

5.6 Reconstruction of the field

Once the field φ_r has been built on the patch areas, it becomes possible to evaluate the value of the continuous field $\tilde{\varphi}$ at any point of the continuous structure in the global co-ordinates. Consider a point located on the border of the structure : one keeps first the values of φ_r on all the areas to which the point belongs. Thus one calculates the weighted average using the following equation :

$$\tilde{\varphi}_{EXP}(x_j, y_j, z_j) = \sum_{r=1}^{m_j} \frac{\varphi_r(x_j, y_j, z_j) / C_j^r}{\sum_{r=1}^{m_j} \frac{1}{C_j^r}} \qquad (18.)$$

where m_j is the number of areas including the point j ; C_j^r is a weighting factor corresponding to the distance between the point and the node which is associated to area r.
The value of the displacement or stress field is then available at any measurement points and more particularly, at any points inside an element like the points of Gauss of the external surface for instance.

6 Advantages of the approach

The alternative of using shape fitting has some attractive major advantages:
- Thanks to the fitting of the experimental field, unmeasured displacement can be estimated. It is now possible to associate an experimental value to every node of the mesh on the measurement surface but particularly, to any point in the element measured face. This allows for the construction of indicators of the errors of discretisation. Moreover, the use of the patch recovery technique makes the process computationally simple.
- In classical updating processes, the expansion by projection of the experimental modes on the base defined by the analytical modes has proven its efficiency. This projection has a smoothing effect on the measurements and makes them more compatible with the analytical solution. Here, the fitting of the measurements by use of polynomial expressions of the same form as those used for the FE analysis has a smoothing effect. They can then be used in numerical calculations, such as updating, without introducing numerical instabilities as sometime happens when using directly the measured data.
- The use of models with six DOFs per node for updating or coupling [20] may require the measurement of the rotational DOFs. They are normally neglected from experimental modal analysis due to the difficulty in measuring them. [19] calculates the two out-of-plan rotations by derivation of a plane fitted in a least-square sense to SLDV measurements.
- The process developed here can be extended to models using shell elements [1].
- With thin structures, when the experimental response set is limited only to out-of-plane translations, the displacement along the two other directions may be evaluated. The measured translations can be associated with the points of the neutral axis and with the assumption of small displacements, the movement in the two other directions can be taken equal to zero. If the structure deformation maintain each section perpendicular to the neutral fibre the displacements can be evaluated anywhere else on the section.
- The approach can be used for any measured field, namely: strain, stress and displacement.
- The fitting tools can be used for the geometrical correlation. A polynomial representation of the FE topology of the measured surface can be build. If the angular position of the measuring axis is expressed in the model's axis (using optical techniques) it is possible to associate at each pixel of the grid displayed by the measurement system its third co-ordinate. Indeed, with isoparimetric elements, the polynomial functions used to express the displacement field are the same as those used for the geometry.
- The process is completely compatible with current FE programs because it uses their inputs and outputs.

7 Correlation between experimental and FE results

A commonly-used technique for estimating the amount of correlation between measured and FE mode-shape vectors is the Modal Assurance Criterion (MAC) defined as follows :

$$MAC\left(\tilde{\varphi}_{\exp},\varphi_{FE}\right)=\left(\frac{\tilde{\varphi}_{\exp}^{T}\ \varphi_{FE}}{\left\|\varphi_{FE}\right\|\left\|\varphi_{FE}\right\|}\right)^{2} \qquad (19.)$$

MAC values give a good idea of the closeness between two different mode-shapes φ_{exp} and φ_{FE}. They oscillate between *0* and *1*. An unitary value means a perfect correlation. The mode shapes have to be rescaled before correlation.

8 Indicators of the errors

The indicators developed in this work are specially intended to the study of mid-size blades. Those are usually modelled by two layers of solid elements (parallelipiped or prism) at degree two. But, only the points on the external skin of the structure are measured. Than, if the structure is of a thin plate-type and if the amplitudes of deformation are small, the following assumption may be done:
- they are no deformation in the thickness;
- the in-plane displacement of points on the neutral fibre are null.
Than the displacements at all the nodes of the elements can be estimated.
The error at one measurement point is defined as: $e(i)=\tilde{\varphi}(i)-\varphi_{h}(i)$ where $\tilde{\varphi}_{h}(i)$ is the experimental fitted field and $\varphi_{h}(i)$ is the experimental or calculated one at the point *i*. If it is the experimental field than the error include the discretisation errors. At an element level an using an energetical formulation the error is:

$$\left(\int_{\Omega_e} e^{T}\ D^{-1}\ e\ d\Omega_e\right)^{1/2}$$ where D is the elasticity matrix.

8.1 Errors in the fitting process

To quantify the accuracy of the fitting process, the discrepancy between each measured value and the fitted one is check. At an element level error must respect:

$$\int_{\Omega_e}\tilde{\varphi}_{\exp}^{N}(x_i,y_i,z_i)-\varphi_{\exp}(x_i,y_i,z_i)\le tolerance,$$ where *N* is the degree of the fitting. *(20.)*

If this error is above a fixed tolerance for an order *N* greater than the degree of the finite elements, this is a first indicator of discretisation problems.

8.2 Discretisation errors

When the fitted field is an acceptable representation of the measurements, it will be used as the reference for all the error calculations. In the following it will be called the measured field.

8.2.1 Errors calculation using the shape functions

Knowing the value of the measured field at the nodes of the elements ($\tilde{q}_{e}$) and at the Gauss points (χ_i) of the external skin of the elements, the following error may be calculated:

$$\left(\sum_{i}^{n} N_e(\chi_i)\,\tilde{q}_e \quad - \quad \tilde{\varphi}(\chi_i) \right) \frac{1}{n} \qquad (21.)$$

This is an indicator of the aptitude of the shape function to represent the experimental field on an element.

8.2.2 Errors calculation using the stresses

The averaged stress value over an element *E* is compared with the averaged stress value of a smaller element *e* build inside. The size of the element is maintained along the thickness of the blade. The error is:

$$\frac{1}{n} \sum_{i}^{n} \quad D\left(\nabla N_E\left(\chi_i^E\right)\right)\tilde{q}_E - D\left(\nabla N_E\left(\chi_i^e\right)\right)\tilde{q}_e \qquad (22.)$$

In the same idea, the shape function can be introduced :

$$\frac{1}{n} \sum_{i}^{n} \quad D\left(\nabla N_E\left(\chi_i^e\right)\right)\tilde{q}_e \quad - D\left(\nabla N_E\left(\chi_i^e\right)\right)(N_E(\chi_i^E)\,\tilde{q}_E) \qquad (23.)$$

8.3 Errors in the parameters of the model

The basic equation for the calculation of the discrepancies between the analytical and experimental field is:

$$e(i) = \tilde{\varphi}_{EXP}(i) - \varphi_{EF}(i) \qquad (24.)$$

where φ is a displacement or a stress field and *i* is a node or any point on an element.

The comparison of the gradient of displacement between the FE solution and the measured one is also a very sensitive indicator.

The indicators of the error may first guide the mesh refinement. Than the essential parameters of the elements showing parametric-type errors may be used in the optimisation loop of the updating process. Those parameters are the classical input of a FE analysis - Young modulus, thickness and the mass per unit of volume – and may be restricted by the manufacturing tolerances.

Their small number and their strong physical meaning should make their optimisation easy since the mesh has been refined in order to be able to represent the measured field.

9 Case study

The process of detection of the different types of errors in a F.E. model has been validated on the example of a clamped plate structure (60 x 90 x 3mm) (***fig. 2***) using a simulated measured field of displacements. The plate is made of steel (Young's modulus = 2.1 10E11 N/m^2). The mode considered is calculated using a very fine FE mesh (154860 DOFs, 9256 elements), in comparison with the one used for the calculations. For the sake of concision a single high frequency mode has been investigated. A complete process should include the whole set of modes over the frequency band of interest.

The calculated mode is perturbed by noise. Its maximum value is equal to 2% of the maximum displacement. The noise is composed with 1% of white noise an 1% of a combination of the two nearest modes.

The simulated defect is a stiffness loss located at point ***D*** (60 x 55) (***fig. 1***). The defect is a 8 x 4 x 3 mm area where Young's modulus has been reduced of only 30 %.

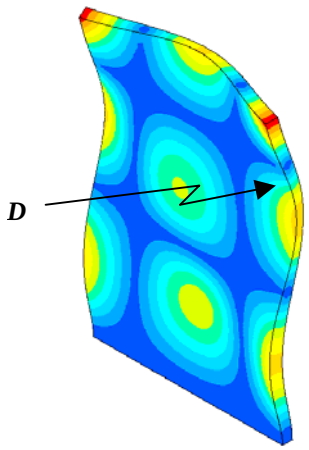

Figure 2: Simulated optical measurements without the added noise, with defect (Mode n° 11 at 12020 Hz - SAMCEF Dynam).

9.1 First F.E. model

A first model made of 400 elements (7080 DOFs) is considered.
The correlation between the smoothed field and the measured one for the 11^{th} mode and for the three measurement directions *x*, *y* and *z* gives MAC values equal to 0.99981,0.99909,0,99994 respectively. Such values should cause the end of the optimisation process of any updating programs based on the MAC.
For a fitting with polynomial function of degree 4, the maximum of the absolute value of the error on the fitting is about 0.037%.

9.1.1 FE mesh discretisation errors

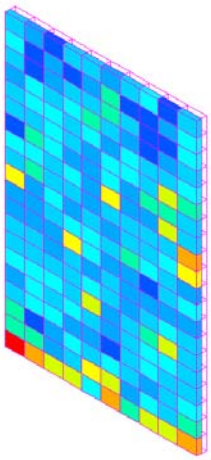

Figure 3: error calculation using equation 22

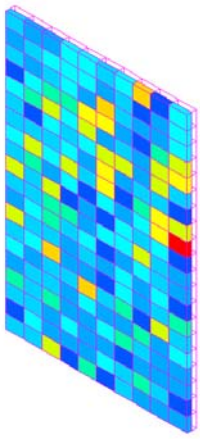

Figure 4: error calculation using equation 23

Results of the procedure for the discretisation error localisation are shown in ***figures 3*** and ***4***.
It can be observed that: - the global mode is not correctly represented;
- the mesh is not sufficiently fine near the clamped edge.

Accordingly, the mesh has to be completely refined.

9.1.2 FE parametrisation errors

The detection of the errors on the parameters indicates (***fig.5*** to ***6***) the presence of an error near the point (60x55) but also errors at the clamped edge.

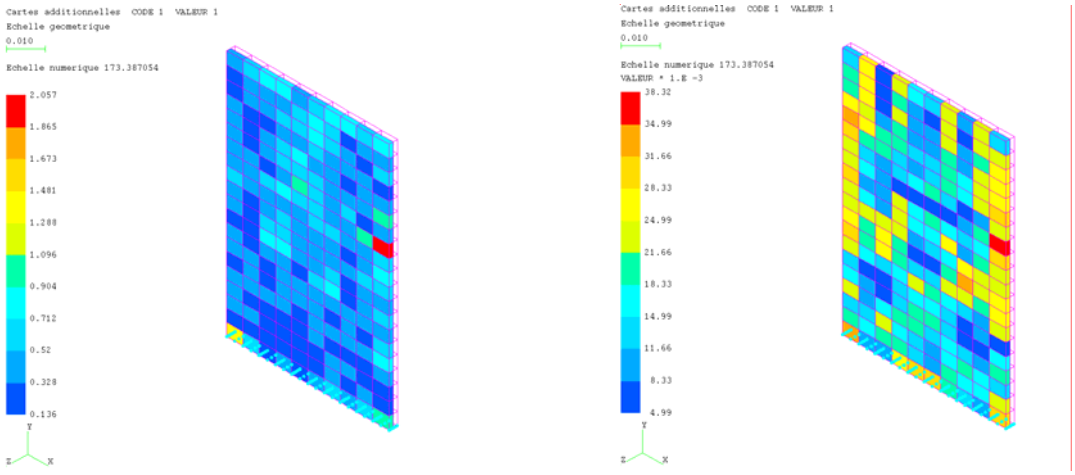

Figures 5 - 6: *error calculation using equation 24*
error on the stress - error on the gradient of displacement

9.2 Second F.E. model

A very basic mesh refinement is realised on the areas where troubles are outlined by the first model (near the point (60 x 55) and near the fixations).The new model has 15912 DOFs for 1200 elements.

9.2.1 FE mesh discretisation errors

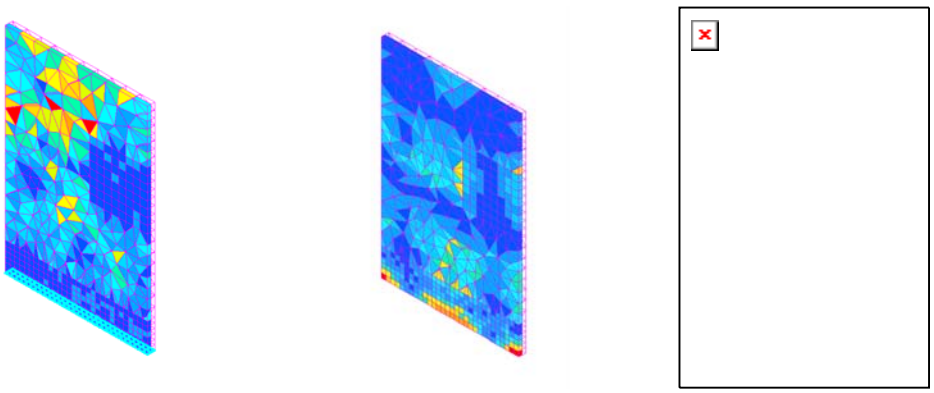

Figures 7-8-9 : *calculation of errors on the discretisation*
- using equation 21 - using equation 22 - using equation 23

A discretisation error is still visible (***fig. 7*** to ***9***) near the clamped end but it is several orders of magnitude lower than the one revealed by the first model. Near the defect, the mesh is good enough and the global mode is correctly represented.

9.2.2 FE parametrisation errors

The error on the elements that have been localised is about 30 % of the absolute value of the three principal components of the stress calculated at the super convergence points of the F.E. elements (***fig.10***).

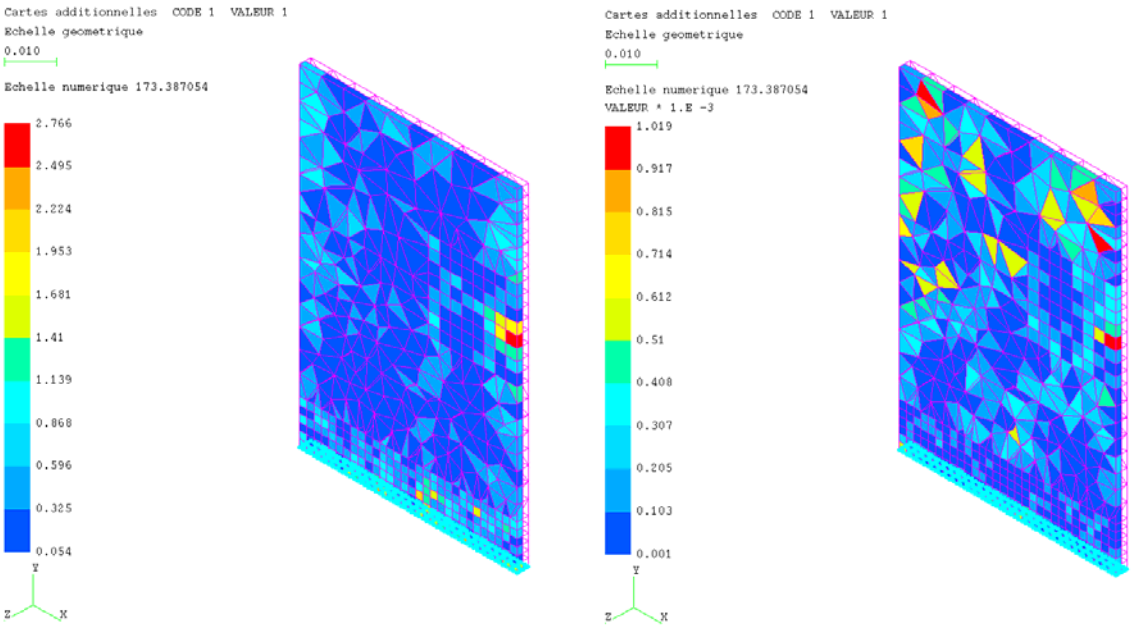

Figures 10, 11 : *error calculation using equation 24*
error on the stress - error on the gradient of displacement

10 Conclusions

The results of field measurement techniques have been exploited for the detection and the localisation of errors in a FE model. The proposed method has been tested using simulated data with noise and has shown its efficiency and its performance. The process has to be completed by :

- taking the whole set of modes into account;
- the use of realistic mesh refinement programs;
- its introduction into an optimisation loop for updating.

The next step will be to validate the method on a compressor blade using true optical data since there may be significant differences between simulated and real measurements. New developments will be focused on :

- the introduction of noise on the geometrical coordinates of the simulated measurement points;
- giving a better meaning to the indicators;
- the study of the effect of the fitting polynomial functions degree, vs the size of the elements, on the reduction of the measurement noise.

The sensibility of the process has already been proven with the detection of errors in a model with a MAC near one.

References

[1] E. M. Boudi, *Analyse de l'erreur de discrétisation pour les éléments finis de coques planes*, Ph. D. thesis, FSA - Ulg, 1996.

[2] P. Collignon, J-C. Golinval, *Comparison of modal updating methods adapted to local error detection*, ISMA 26, p. 1033-1043,Leuven, 1996.

[3] E. Dufeu, *Calcul d'erreur et adaptation de maillage en 3 dimensions*, Ph. D. thesis, FSA - Ulg, 1997.

[4] L. Humbert, *Recalage des modèles éléments finis à partir de mesures vibratoires*, Ph. D. thesis, Ecole centrale de Lyon, 1999.

[5] J.F. Imbert, *Analyse des structures par éléments finis*, Editions Cepadues, France.

[6] R. Pascual, *Model based structural damage assessment using vibration measurements*, Ph. D. thesis, FSA - Ulg, 1999.

[7] Ramsay A.C.A., Sbresnyh, *Some studies of error estimator based on patch recovery scheme*, Finite elements news, issue N 2, p. 13-31, 1994.

[8] M. Geradin, D. Rixen, *Mechanical vibrations*, John Wiley & Sons Ltd, second edition, 1997.

[9] J. S. Slepicka, S. C. Soyoung, *Holographic Diffraction Velocimetry for Measurement of Three-Dimentional Velocity Fields*, AIAA Journal, Vol. 35, No. 7, Jully 1997, p. 1201-1203.

[10] E. Foltête, J. Piranda, J-L. Raynaud, *Quantitative Dynamical Measurements for Model Updating Using Electronic Speckle Interferometry*, IMAC 2001, p. 1305 – 1310.

[11] T.E Purcell, *Dynamic Stress Analysis Of Gas Turbine Rotor Airfoils Using Thermoelastic techniques*, SEM – Experimental techniques, May/June 1996, Vol. 20, No. 3

[12] B.Dierckx, H. Klingele, H. Van der Auwerear, J. Leuridan, *Holography as s Quantitative Modal testing Technique Applied to a Brake Drum in View of Correlation With FE Data*, IMAC 1996, p. 783 – 789

[13] M. J. Sunderaresan, P. F. Pai and al.,*Damage detection on a Wind Turbine Blade Section*, IMAC 99, p. 1359 – 1365.

[14] M. Martarelli, G.M. Revel, C. Santolini, *Automated Modal Analysis by Scanning Laser Vibrometry : Problems and Uncertainties Associated With The Scanning System Calibration*, Mechanical Systems and Signal Processing, 2001, p.581 – 601.

[15] Etmeyer

[16] R. Krupka, A. Ettemeyer, *Brake Vibration Analysis With Three-dimentional Pulsed ESPI*, Experimental Techniques, March/April, 2001.

[17] P. Avitabile, *Model Updating – Endless Possibilities*, Sound and Vibration, September 2000.

[18] P.Slagen, Y. Lion, J-C. Golinval, M. Géradin, *Modal Analysis of Plate Structures Using Digital Speckle Pattern Interferometry*, IMAC 95, p. 1192 – 1197.

[19] M.J. Ratcliffe, N.A. Lieven, *Measuring Rotational Degrees of Freedom Using a Laser Doppler Vibrometer*, Journal of vibration and acoustics, January, vol. 122, 2000.

[20] M.L.M. Duarte, D.J. Ewins, *Some Insight Into the Importance of Rotational Degrees-of-Freedom and Residual Terms in Coupled Structure Analysis*, IMAC, p. 164 – 170, 1995.

[21] D. Simon, J-C Golinval, *Finite Element model updating based on Hologaphic and Speckle Interferometry Measurements, PHOTOMEC'99 - BSMEE, 1999.*